Investigating Dynamic Response of a Buried Pipeline in Sandy Soil Layer by 1G Shaking Table Test

F. Jafarzadeh[1] , H. Farahi Jahromi[2] and E. Abazari Torghabeh[3]

Received: June 2009 Accepted: March 2010

Abstract: *Investigating the parameters influencing the behavior of buried pipelines under dynamic loading is of great importance. In this study the soil structure interaction of the pipelines with the surrounding soil was addressed using shaking table tests. Wave propagation along the soil layers was also included in the study. The semi infinite nature of the field was simulated using a laminar shear box. The soil used in the experiments was Babolsar coastal sand (Iran). PVC pipes were used due to their analogy with the field. Eight models were constructed with the first four models having uniform base. In the next models, the non-uniformities of real ground were simulated using a concrete pedestal installed at the very bottom of the shear box. Pipe deformations under dynamic loading, acceleration distribution in height, soil settlement and horizontal displacements were measured by strain gauges, acceleratometers and displacement meters. Analyzing the obtained data, influence of different parameters of dynamic loading such as acceleration, frequency, soil density, base conditions and shaking direction to pipe axis on the acceleration amplification ratio and pipe deformation were investigated. Also in order to study the effect of dynamic loading on two different materials, soil and pipe, the horizontal strains were compared.*

Keywords: *Buried pipe, Shaking table test, Laminar shear box, Sand, Strain*

1. Introduction

Buried pipelines functioning as transmission lines of energy are drastically devastated when exposed to dynamic loading conditions such as earthquakes. The dynamic behavior of buried pipelines has been the area of research over the last five decades. This intensive work in this area has led to massive experimental and analytical studies. These investigations show that different types of damage might occur in the buried pipelines including buckling, torsion, tension and compression of the pipes. Furthermore the joints crush, separation of the pipe and the supporting blocks, replacement of the manholes and longitudinal fissure induction on the pipe are among the other failure modes which might cause severe damages to the pipelines during dynamic loading. Considering the aforementioned studies, six aspects of the damages to the pipelines are summarized as follows:

1. 1. Faulting Effect on Pipe Response

Several studies were conducted on the dynamic response of the pipelines intersecting a fault. Ariman and Lee [1] conducted some experiments to study the bending – tension response of the pipe when intersected by a fault. The results showed that the angle of intersection did not have a significant impact on the bending strains. It was also shown that any approach to decrease the soil structure friction would reduce the strain levels induced in the pipe and consequently increase the stability of the pipe. Furthermore, any decrease in the buried depth of the pipe in the intersection area would result in a considerable decrease the compression-tension strains on the pipe.

In another study Tohada et al. [2] developed an apparatus to model the topographical changes as well as the bedrock non-uniformities on the pipe. In that study, six different conditions were simulated, to cover various conditions of soil-rock-pipe intersection.

In addition, an apparatus was devised in a way to change the supporting conditions to model the plane strain situation. It was shown that the

* *Corresponding author. Email: email: fardin@sharif.ir*

1 *Associate Professor, Civil Eng. Dept., Sharif University of Technology, Tehran, Iran.*

2 *PhD Student, Civil Eng. Dept., Sharif University of Technology, Tehran, Iran.*

3 *PhD Student, Civil Eng. Dept., the University of Alberta, Canada.*

acceleration recorded at the two ends of the pipe is higher than the middle point which illustrates the significance of the joints as compared to the middle parts of the pipeline. Various topographical cases were simulated using an aluminum box in a soil container. As shown in Figure 1, the bedrock conditions 1 and 4 induced bigger strains than the models 2 and 3 revealing the fact that any sudden change in the stiffness and thickness of the underlying soil can cause severe damages to the pipeline.

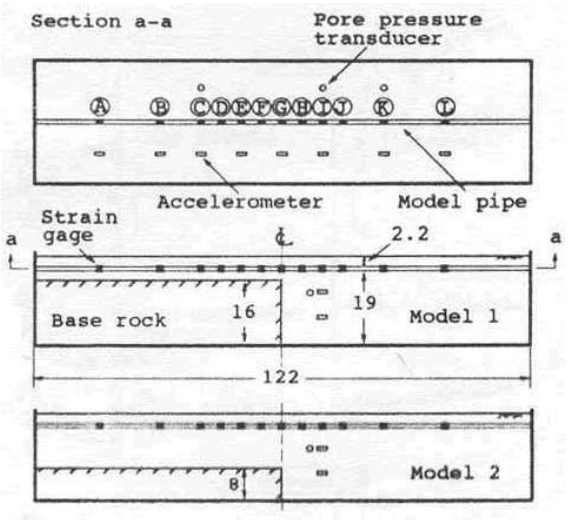

Fig.1. The simulation of non-uniformities in soil [2]

1. 2. Pipe Behavior under Liquefaction Process in Sand

Miyajima et al. [3], conducted some experiments to study the effect of liquefaction on the failure behavior of the pipelines. In their experiments, a new drainage system was developed using a gravel wall as well as a pile to prevent the liquefaction occurrence in the soil.

Towhata et al. [4] performed several tests using shaking table to measure the force which is needed for dragging a pipe with constant velocity before and after dynamic loading application.

It was eventually found out that the frequency of the excitation and the density of the soil did not have a significant influence on the force recorded. The research showed that the ratio of the drag force exerted on the pipe after and before liquefaction is 30 to 1.

Moreover Kiku et al. [5] showed that the sub-grade horizontal reaction modulus could decrease to 5% compared to the situation prior the liquefaction occurrence. Furthermore, Yanagimoto et al. [6] introduced a new method to evaluate the critical proportional displacement between pipe and soil to reach a maximum load in a pipe. Conducting several dynamic tests, they showed the trivial effect of loading period on the pipe response. Another study performed by Yasuda et al [7], concluded that some effective parameters including the density of the soil and the pipe, water table level, soil gradation as well as the pipe section should be taken into account in the design procedure.

1. 3. The Pipe Dimension Effect on Damages

In 1994, several experimental tests were done by Bardet and Davis [8] to address the behavior of large diameter pipes subjected to dynamic loading. Various diameters with different base conditions were used in the experiments. It was shown that the pipes having larger diameters experienced higher strains and damages easier than the others. Also the peak ground velocity was concluded to be the key parameter for assessment of damage to the structure. However, the ground displacement on its own can be considered an important factor to cause the damages.

1. 4. Case Studies to Assess the Damage and its Process on the Pipelines

O'Rourke and Palmer [9] performed a review on the damages induced on the pipes in 11 famous earthquakes and proposed several methods in manufacturing the pipes and welding process. In-addition Hamada [10] evaluated the damages in lifelines in Japan. Through his research he proposed two methods for computing the devastation in numerical calculations by counting parameters like: the ground situation, liquefaction occurrence, pipe type, displacement recorded due to earthquake and the strain and stress induced on the pipe.

1. 5. Comparing the Results of Analytical Studies and Experimental Tests

Mohri et al. [11] compared the results recorded in experimental tests using the shaking table

device with the outcomes from FLIP program. They concentrated on water uplift pressure effects on the pipe in liquefaction stage and introduced a critical depth which separated 2 buckling failure mode, local (shell) and general (along the length).

1. 6. Developing failure criteria for buried pipes used

Several case studies associated with the buried pipelines in urban areas were reviewed by o'Rourke and Liu [12] resulting to the fact that the buckling mode of failure is more likely to damage the pipeline than the bending mode. They proposed a critical length to separate the two failure modes. They also concluded that if the ground displacement happens above the critical length, buckling failure will take place.

In this paper four major issues were selected to be addressed by conducting several 1g physical model tests. These parameters are: effect of bedrock on pipe, effect of loading direction with respect to the pipe axis, dynamic loading characteristics on pipe and finally the effect of soil density.

2. Test Aparatus and Model Preparation

2. 1. Shaking Table Device

The 4x4 m shaking table device in Sharif University of Technology was used to induce the desired excitation to models. The Table has 3 degree of freedom in x, y direction and rotation around the x-y plane vector with the maximum displacement of 250 and 400 mm in x and y direction; respectively. Also, it can sustain a model up to 20 tons weight.

2. 2. Shear box

A laminar shear box designed in Sharif University [13] includes 24 aluminum layers; each having the dimensions of 100x100x 4 cm. In order to reduce the friction between the layers and to simulate the displacement of soil layers, 12 ball bearings were used between the two adjacent layers. There are a variety of equipments comprising the laminar shear box as shown in figure 2. Among them, are a saturation-drainage system, horizontal supporting columns, the crossing elements on the top and horizontal displacement controlling planes between layers to prevent the movement in desired direction (Fig.2).

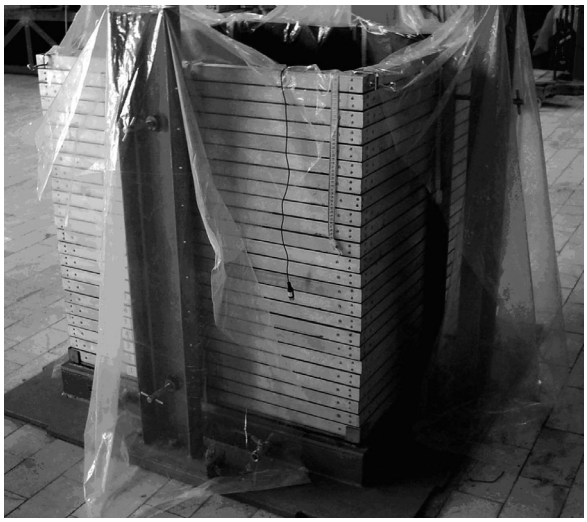

Fig.2. Laminar shear box

2. 3. Soil Characteristics

Uniform sand provided from Babolsar shores and named Babolsar sand was used in this study. The main index properties of this uniform sand is summarized in Table (1) and the gradation curve for five samples of this soil are shown in Figure (3).

2. 4. Pipe Characteristics

Among three different options available for type of the pipe including steel, tin and PVC, the

Table 1. Main Index Properties of Babolsar sand

Sample Classification	Gs	D_{50} (mm)	γ_{min} (grf/cm^3)	γ_{max}(grf/cm^3)
SP	2.65	0.2	1.508	1.726

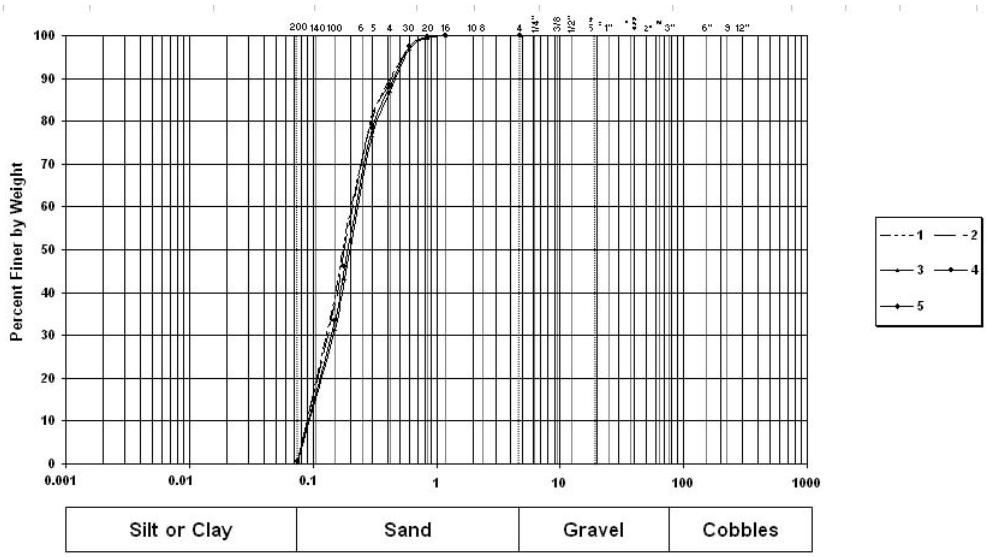

Fig 3. Gradation curves for five samples of Babolsar sand

latter option was chosen due to its simplicity and ease in use as well as its flexibility when subjected to dynamic loading. The pipe had 80 cm length, 5.8 cm inner diameter and 0.178 cm thickness with E and υ equal to 18500 kg/cm^2 and 0.3; respectively.

2. 5. Model Preparation

2. 5. 1. The Desired Density in Sand

In order to obtain the desired relative density which was less than 25%, some calibration tests were required to be done. Sand pluviation was performed using three different sieves to see the effect of sieve size on the relative density. It was finally concluded that sieve #4 would give closer results to the desired relative density compared to that of sieve #10 and #20. Applying this method, the sand was poured from a rigid pouring bucket with sieve #4 in the bottom. The optimum height from which the sand was poured, was in the order of 20 to 25 cm. Figure 4 shows the sieve installation as well as the sand pluviation in the preparation stage.

2. 5. 2. Simulating the topographical conditions of the pipe base

One of the significant aspects of the dynamic behavior of the pipeline systems is the base condition of the ground on which the pipeline is located. The non uniformities of the bedrock were

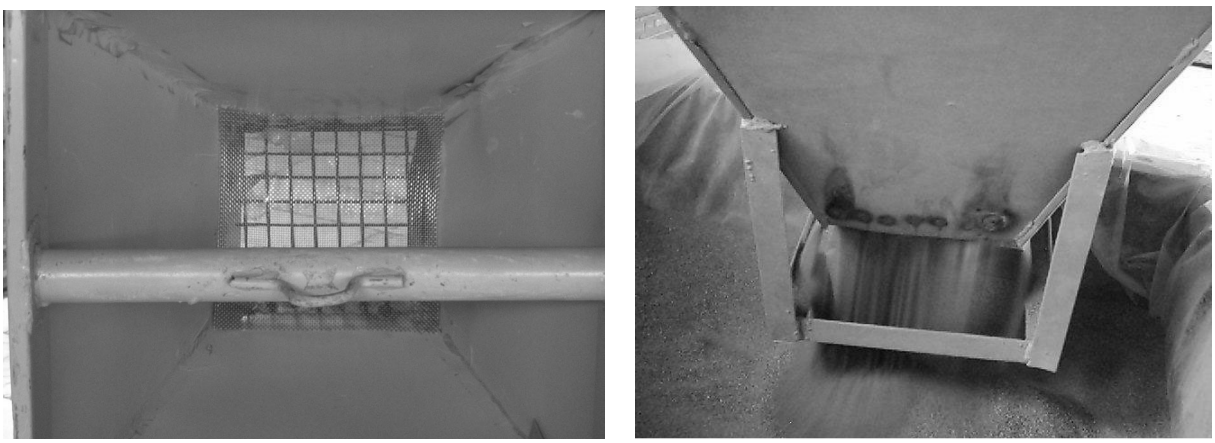

Fig.4. Soil pouring in the shear box using the bucket

simulated by providing a cast concrete pedestal with a parallelogram cross-section depicted in Figure 5. The concrete pedestal has a length of 95 cm, height of 17 cm and width of 50 cm and was carefully placed in the soil container. Thus, the experiments were divided into two major categories. In the first series, the concrete pedestal was not used for simulating a uniform condition of pipe trench while in the second series, of tests the concrete pedestal was placed in the model to simulate the existence of the bedrock.

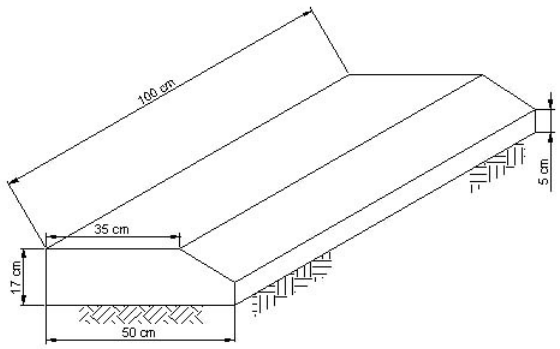

Fig. 5. Pedestal cross section

2. 5. 3. Fixing of the Buried PVC Pipe in the Shear Box

For the first group tests, in which the concrete pedestal was not used, the pipe was fixed between two bearings shown in Figure 6. By making a 5 cm diameter hole in each support with the depth of 5 cm, a semi rigid fixation was provided to serve as long buried pipe (Figure 6). In models having the concrete pedestal fixed in the shear box, one end of the pipe was remained unchanged; while, the other was fixed on the pedestal. Figures 7 and 8 show the details of the connection.

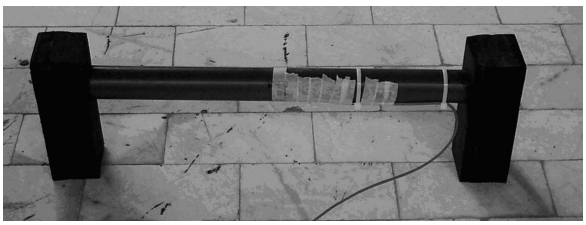

Fig. 6. The buried pipe and its two supports in first model group

2. 5. 4. Instrumentation

Several different measuring instruments were used in the experiments to better monitor the behavior of the soil and pipe. The devices installed in the model include accelerometers, LVDT's and strain gauges. Five strain gauges were installed on the pipe as shown in Figure 9. Three LVDT's were placed in 20, 40 and 60 cm from the base of the shear box to measure the horizontal displacements of the layers. In order to measure the settlement of the soil subjected to dynamic loading on LVDT was placed on top of the model. Where the concrete pedestal was not used, the accelerometers were mounted in 0, 20, 40 and 60 cm from the base. In the other set of experiments where the concrete pedestal was used, one accelerometer was placed on the base, two on 20 cm from the base, one on the soil and the other on the

Fig. 7. Fixing the head of the pipe on the pedestal

Fig. 8. The buried pipe and pedestal support in the shear box

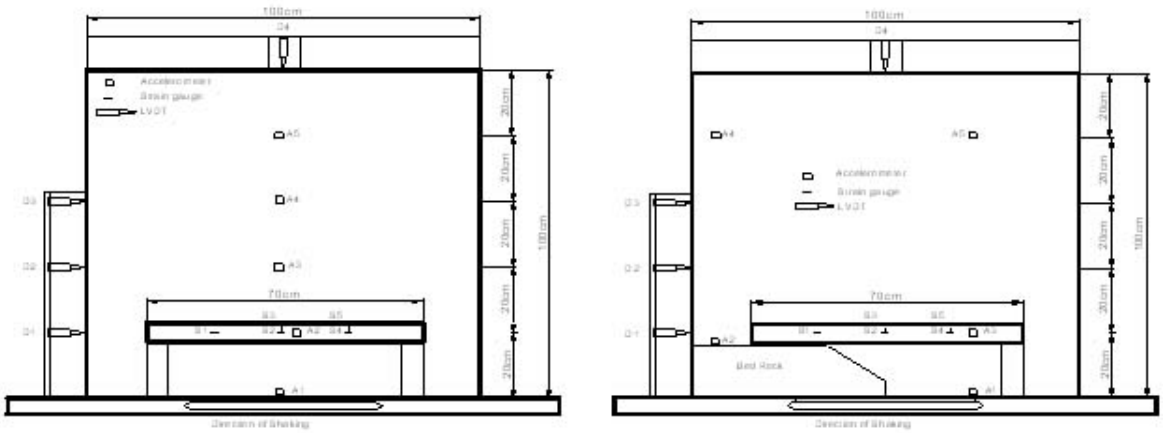

Fig. 9. Schematic cross section of the models and positioned sensors: (a) without pedestal and (b) with pedestal

bedrock. The last accelerometer was placed on 80 cm high from the base. The instrumentation deployment is illustrated in Figure 9.

2. 5.5. Model Preparation for Dynamic Loading

Using the above mentioned method for model preparation, eight models were prepared. Figure 10 shows the arrangement of pipe, sensors and sand in the shear box during model construction.

3. Experimental Program

3. 1. Dynamic Loading Characteristics

The models prepared are divided in two major groups, with and without the concrete pedestal, which acts as a bedrock in the model. Therefore, the loading plan was designed in a way that the results recorded from these two model groups could be compared. In addition, according to the loading direction to pipe's axis, each model loading are divided in two minor sets. The loading direction which could be parallel or perpendicular to the axis, revealed the buckling and bending failure condition, respectively. The dynamic loading which excited the models are sinusoidal acceleration with amplitude in the range of 60 to 1100 gal, the frequency of 5 or 10 HZ and the number of cycles of 10, 20 and 40. Table 2 summarizes the loading characteristics and model properties before and after each test.

4. Test Results

With reference to Table 2, eight models were prepared and subjected to dynamic excitations. The data obtained from data acquisition system

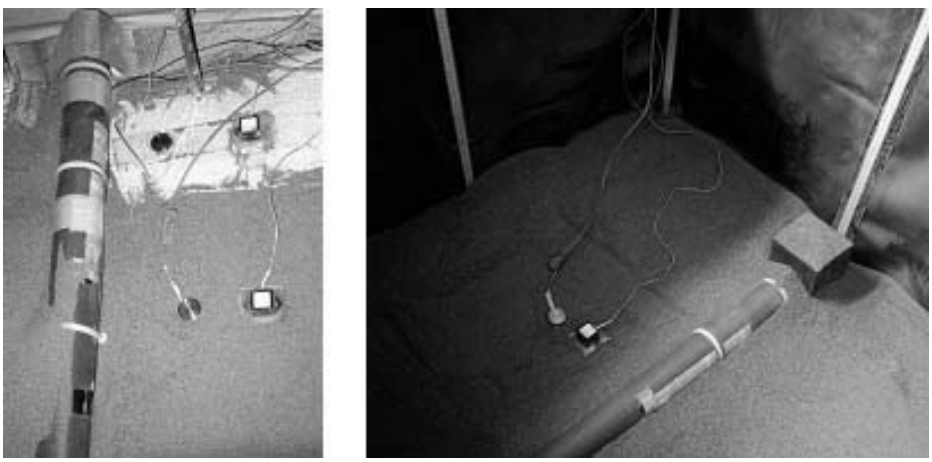

Fig. 10. Filling the box up to pipe level (20cm) and placing the sensors in shear box (for two model groups :a-with and b-without the presence of pedestal)

Table 2. Dynamic Loading characteristics and model properties before and after the tests

Model	Number of	Initial Dr	Loading	Pipe	Final Dr	Remarks
1	10	28.4	Harmonic	Bending	96.2	No Pedestal
2	17	16.0	Harmonic	Bending	90.7	No Pedestal
3	20	8.6	Harmonic	Buckling	92.7	No Pedestal
4	23	7.0	Harmonic	Buckling	92.9	No Pedestal
5	31	13.2	Harmonic	Bending	81.5	With Pedestal
6	32	11.0	Harmonic	Buckling	88.4	With Pedestal
7	12	8.2	Harmonic	Buckling	76.6	With Pedestal
8	15	9.2	Harmonic	Bending	80.3	With Pedestal

were converted to physical parameters such as acceleration, displacement and strains. Figures (11) and (12) demonstrate the typical recorded results for acceleration on the base, on the pedestal, near the pipe and 60 or 80 cm high in the soil, the displacement of the soil layers at the pipe elevation and the strains related to strain gauges No. 1 to 5 on the pipe. It is emphasize that Figure (11) is pertinent to models in which pedestal were not used, however results presented in Figure (12) were obtained from the models with pedestal.

5. Discussion

5. 1. Acceleration Amplification Ratio

As the shear wave is introduced to the base of the model, the energy of the wave is dissipated by the soil grains. In order to study the shear wave distribution pattern in the model a simple

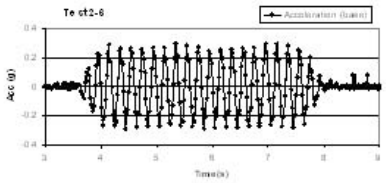

(a). Base acceleration (A1)

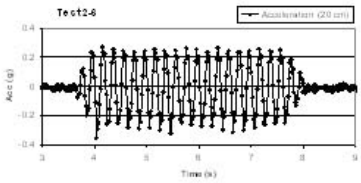

(b). Acceleration near to pipe (A2)

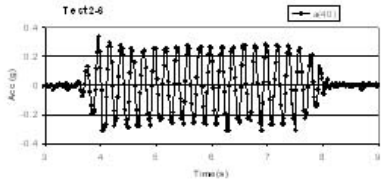

(c). Acceleration of the soil in 40 cm height (A3)

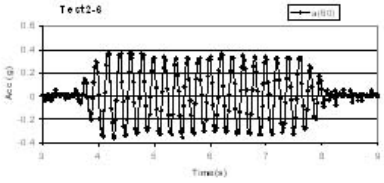

(d). Acceleration of the soil in 60 cm height (A4)

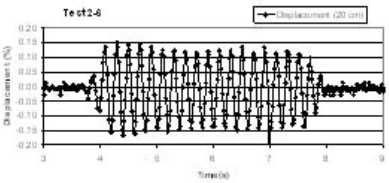

(e). Soil displacement at 20 cm high (D1)

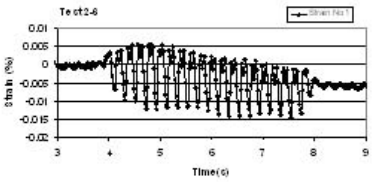

(f). Longitudinal Strain measured at the 0.25L of the pipe (S1)

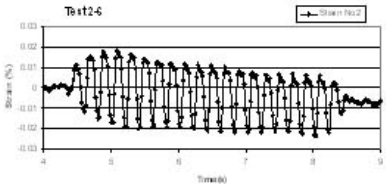

(g). Longitudinal Strain measured at the mid length of the pipe(S2)

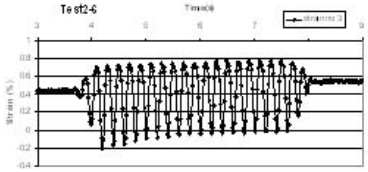

(h). Peripheral strain measured at the 0.25L of the pipe (S5)

Fig. 11. Recorded acceleration and strain time histories in soil and pipe for Test 2-6 at different points without pedestal

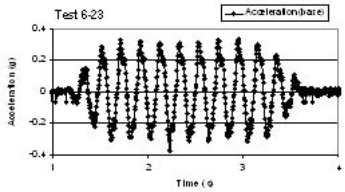

(a). Base acceleration (A1)

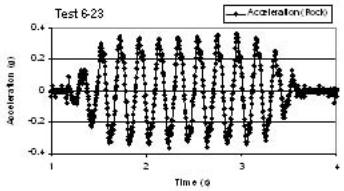

(b). Acceleration on the concrete pedestal (A2)

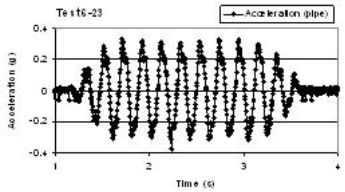

(c). Acceleration near the pipe (A3)

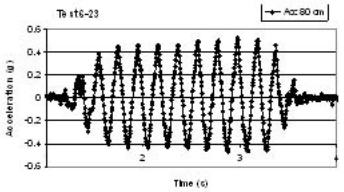

(d). Soil acceleration in 80 cm height (A5)

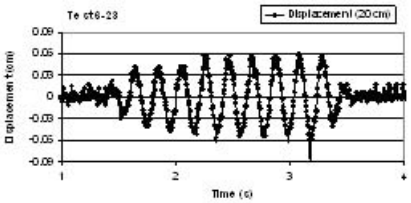

(e). Soil displacement at 20 cm high (D1)

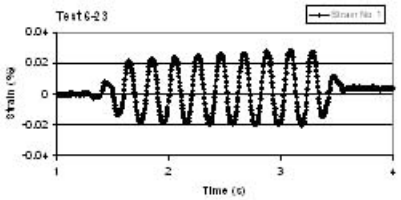

(f). Longitudinal Strain measured at the 0.25L of the pipe (S1)

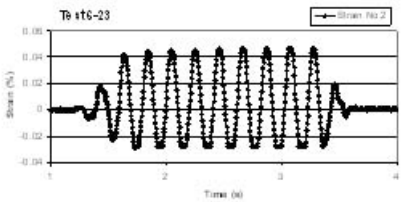

(g). Longitudinal Strain measured at 0.5L of the pipe (S2)

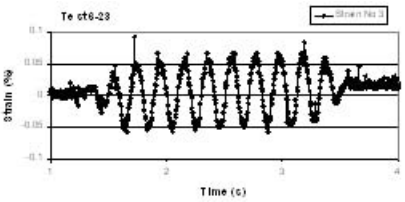

(h). Peripheral Strain measured at the 0.5L of the pipe (S3)

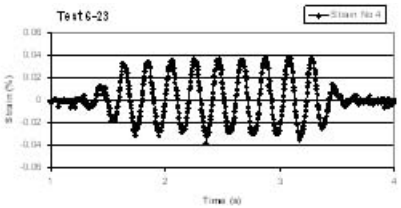

(i). Longitudinal Strain measured at 0.75L of the pipe (S4)

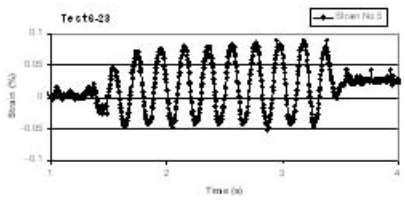

(j). Peripheral Strain measured at the 0.75L of the the pipe (S5)

Fig. 12. Recorded acceleration and strain time histories in soil and pipe for Test 6-23 at different points with pedestal

parameter known as ratio of acceleration amplification (Raa) is defined and applied in the analysis of wave distribution. Raa is the ratio of amplitude of recorded acceleration in soil or pipe to the applied acceleration at the base level.

Figures 13 and 14 show the models without the pedestal while in Figures 15 and 16 the same parameter is calculated for the models containing pedestal. The effect of placement of the pedestal in the model has been thoroughly investigated using the amplification ratio in the two sets of models.

As it can be seen from Figure 13, the increase in the soil density does not have any considerable influence on the Raa. However any change in the base acceleration can make a significant change on Raa. (Figure 14). In the next four figures the Raa for models with concrete pedestal was depicted. Similar to previous diagrams the Raa value is not considerably affected by relative density of soil, alternatively, the effect of base acceleration on this parameter cannot be ignored. Ascending base acceleration resulted in smaller quantity for Raa.

Figure (19) compares the Raa values for the models with and without pedestal. It can be observed that the Raa values belong to models with pedestal are not dependant on base acceleration and are near to one; However, in models without the concrete pedestal, Raa is a function of the base acceleration indicating that low acceleration in the base has been amplified in the upper layers. Furthermore, if the base consists of different materials having different rigidities, the soil-rock interaction will amplify the acceleration of the above layers. In Figure 20, the effect of soil density on Raa has been illustrated and it has been shown that the density of the soil sample does not make a drastic change in the accelerations induced in the upper layers.

One of the important parameters which should be considered in pipeline design is the topography of the medium through which the pipeline is passing. For instance, the relative rigidity of the two adjacent media which the pipe is passing through must be taken into consideration. This situation is depicted in Figure 21 in which the acceleration on two points on the bedrock and the soil have been monitored. Comparing the results show that the more rigid the base the higher Raa will be. This phenomenon reveals to consider a higher safety factor in design method where the pipeline goes over the stiff materials.

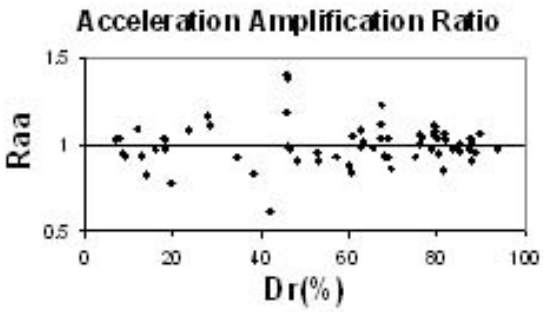

Fig. 13. Raa versus Dr for models without pedestal (A2/A1)

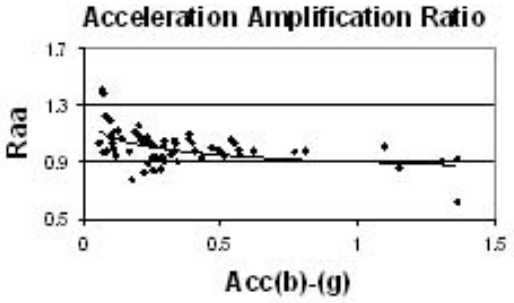

Fig. 14. Raa versus base acceleration for models without pedestal (A2/A1)

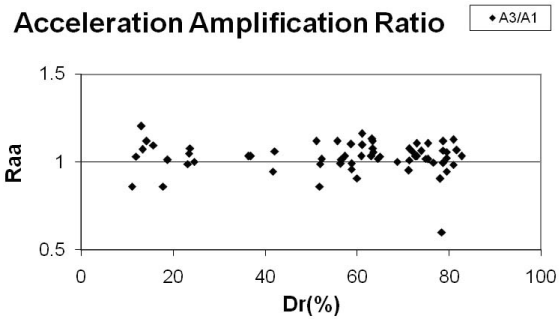

Fig. 15. Raa (pipe/base) versus Dr for models with pedestal (A3/A1)

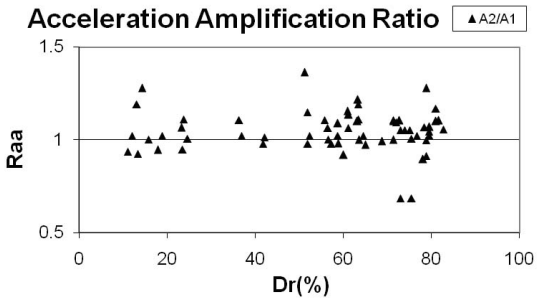

Fig. 16. Raa (rock/base) versus Dr for models with pedestal(A2/A1)

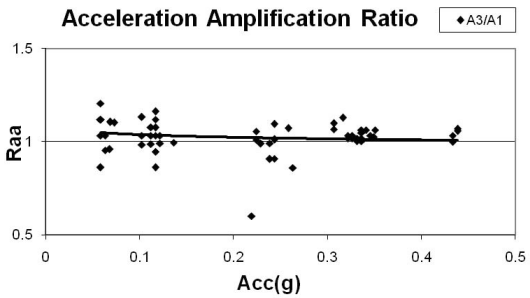

Fig. 17. Raa (pipe/base) versus base acceleration in models with Pedestal

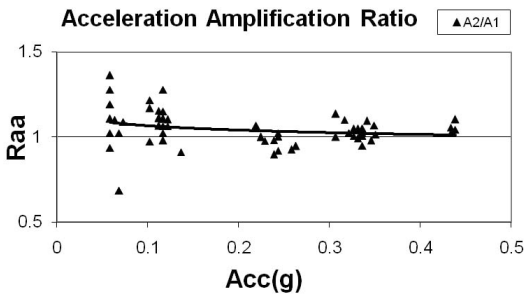

Fig. 18. Raa (rock/base) versus base acceleration in models with pedestal

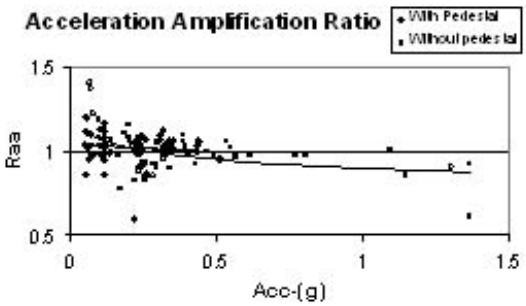

Fig. 19. Raa (pipe/base) for models with and without pedestal

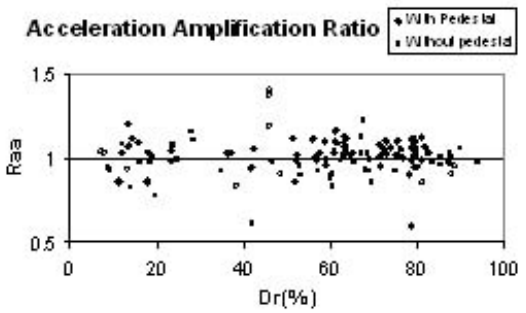

Fig. 20. Raa (pipe/base) versus Dr for models with and without pedestal

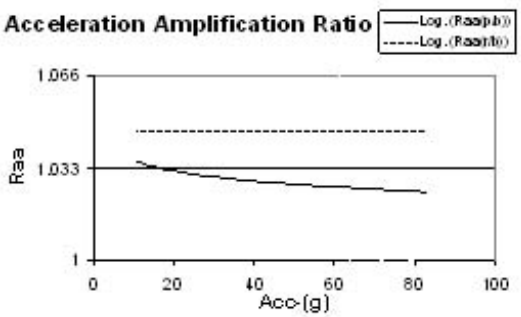

Fig. 21. Comparison of Raa versus base acceleration for two near points in soil and on rock for models with pedestal

5. 2. Acceleration Effect on the Pipe Strains

As mentioned before, the strains measured consist of both longitudinal and circumferential ones. Calculated strains which are shown in Figures 22 to 25 indicate that increasing acceleration will lead to higher strains. This inference is clear for both loading modes (perpendicular and parallel) in any frequency in all tests.

It can be seen in Figures 22 and 23 that all the strain points related to 0.3g acceleration are above the strains related to 0.1 g excitations. Also, the Figures 24 and 25 which show the circumferential strains confirm the above inference. Without considering the relative density and its effect on the strains in these two shapes, the increasing trend of the strain points with higher values of acceleration could be concluded.

5. 3. Effect of Loading Direction to Pipe Axis on the Strains

During the tests, dynamic loading is applied parallel and perpendicular to the pipe axis. Thus the effect of the loading direction can be verified by comparing the strains in the two sets of experiments. Figures 26 and 27 summarize the data associated with the longitudinal strains having 5 Hz frequency and accelerations 0.3g to 0.5g. In the next four figures, 28 to 31, the strains of the models containing the concrete pedestal have been depicted. It can easily be observed from these figures that the buckling mode of failure is dominant in models containing the concrete pedestal which causes higher strains in the pipe. This conclusion however cannot be made in models without the concrete pedestal.

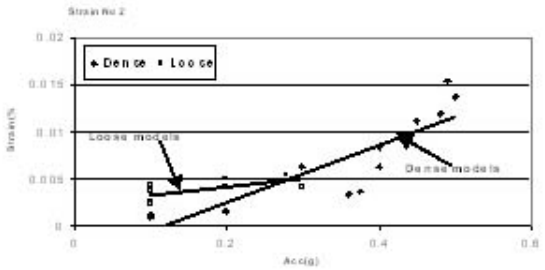

Fig. 22. Acceleration effect on pipe strain, f=5 Hz, Buckling mode without bedrock (S2)

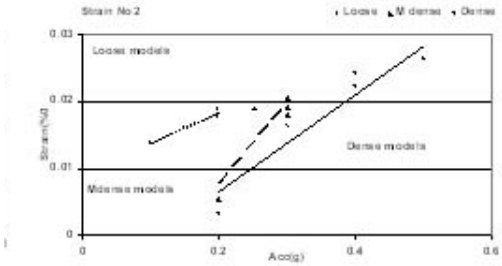

Fig. 23. Acceleration effect on pipe strain,f=5 Hz, Bending mode without bedrock (S2)

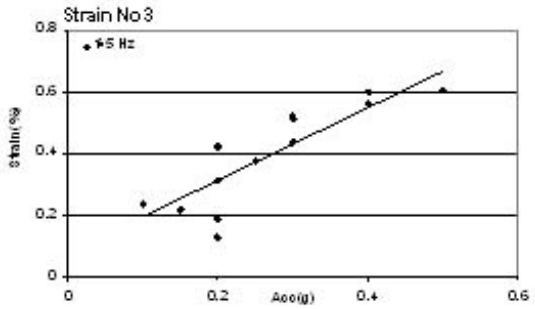

Fig. 24. Acceleration effect on pipe strain, Bending mode without bedrock (S3)

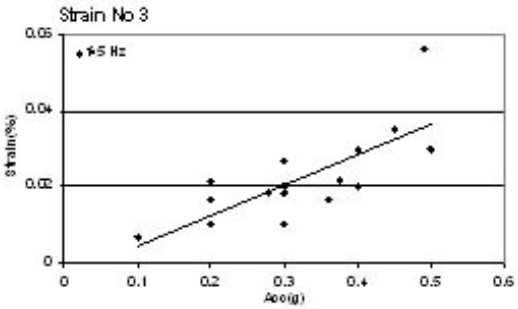

Fig. 25. Acceleration effect on pipe strain, Buckling mode without bedrock (S3)

Therefore, it is concluded that in areas where the trench base is composed of uniform soil, the perpendicular direction is more likely to cause failure. Unlike the previous case, the rigid rock movement parallel to the pipe axis caused higher strains in the buckling mode than the bending one. It is then concluded that in models with the uniform base consisting of flexible material, the bending mode should be considered critical.

Figures 32 to 34 summarize the results for circumferential strains measured at the mid length of the pipe. Similar to previous results, in this mode in which the peripheral strains are the considered subject, the bending mode of loading caused the critical conditions to the pipe. It means that the pipe is likely to be damaged more in loading perpendicular to pipe axis than the parallel direction. In opposition to previous case in which a general statement could not be presented, in the case of circumferential strains it can be said that for all conditions of foundation and loading, including the acceleration and frequency, the perpendicular loading results in greater strains than the parallel one. The reason behind that is in loading direction parallel to the pipe axis, the pipe is subjected to compression-tension stress cycles while the main body of the pipe is kept undisturbed. Thus, it is concluded that the loading mode perpendicular to the pipe axis would be the critical failure mode which

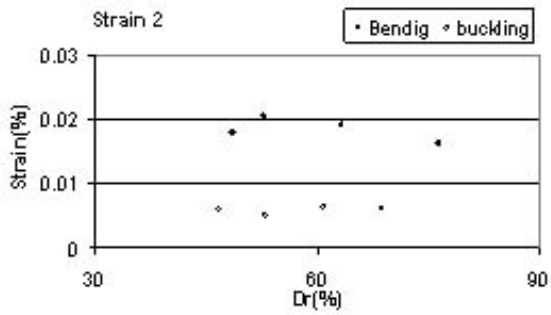

Fig. 26. Loading direction effect, f=5HZ without pedestal, a=0.3 g

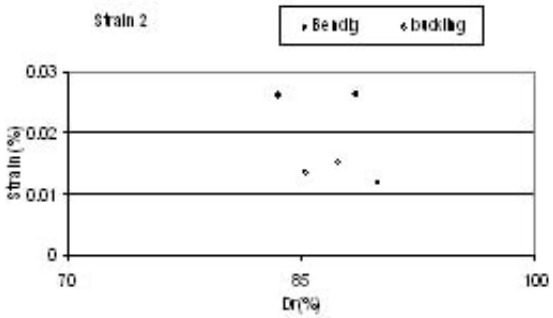

Fig. 27. Loading direction effect, f=5HZ, without pedestal, a=0.5 g

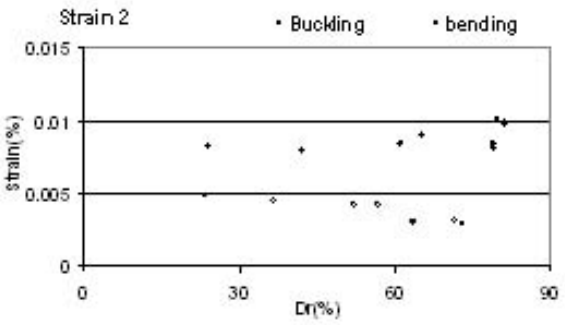

Fig. 28. Loading direction effect, f=5HZ with pedestal, a=0.1 g

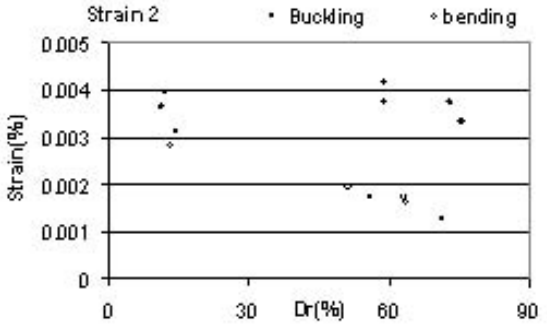

Fig. 29. Loading direction effect, f=5HZ, with pedestal, a=0.3 g

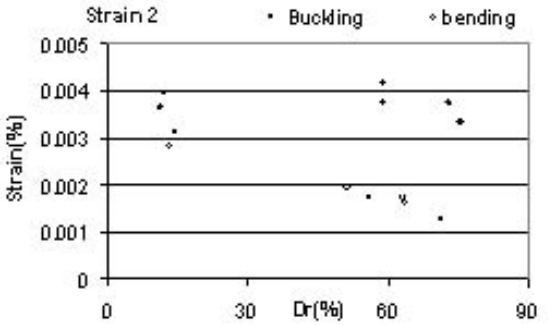

Fig. 30. Loading direction effect, f=10 Hz with pedestal, a=0.1 g

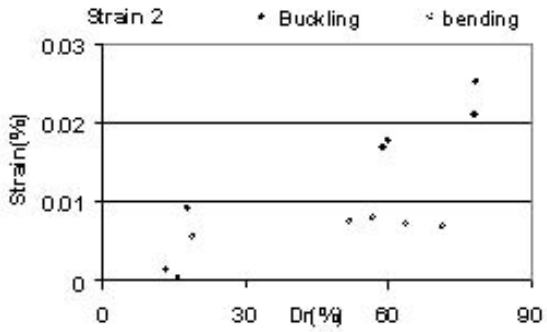

Fig. 31. Loading direction effect, f=10 Hz, with pedestal, a=0.3 g

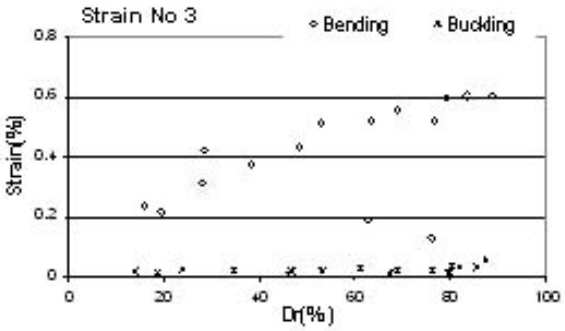

Fig. 32. -Loading direction effect- f=5 Hz ,a=0.1-0.5g without pedestal

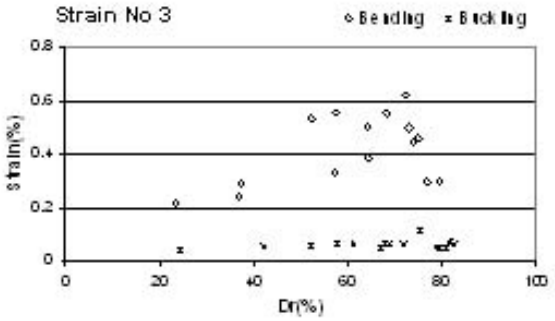

Fig. 33. Loading direction effect f=5 Hz-a=0.3-0.4g with pedestal

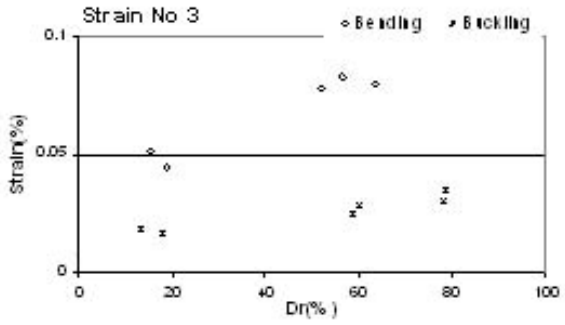

Fig. 34. Loading direction effect, f=10 Hz, a=.24 g, with pedestal

significantly deforms the pipe cross section.

5. 4. Effect of Concrete Pedestal on Pipe Strains

As mentioned previously, the concrete pedestal was placed in the model to simulate the effect of non-uniform base conditions on the pipe response. In case of parallel loading to pipe axis, the longitudinal strains induced on the pipe were higher for the model with pedestal than the other case. Figures 35 and 36 show the results for this

condition. Also, Figures 37 and 38 which belong to 5 and 10 Hz frequency loading, confirm the above mentioned judgment.

Regardless to acceleration values induced to models in Figure 39 the models with pedestal resulted in higher peripheral strain in mid length of the pipe (strain No. 3). This conclusion is also true for Figures 40 to 42. The strain values for 240 gal acceleration loading and 10 Hz frequency in any relative density was higher in model with pedestal than the ones which resemble the uniform base conditions.

Despite the above results for buckling mode of loading, the recorded strains for the bending mode in strain gauge No. 2 were not as clear as the previous are. So an apparent result cannot be seen for this case. This uncertainty also remains for the strain No. 3. This means that the buckling mode presents an obvious result; however, for bending mode the strains for two cases are not so clear to yield in an incisive result. In Figures 43 and 44 the recorded strains in bending mode which are in contrast to previous result are shown.

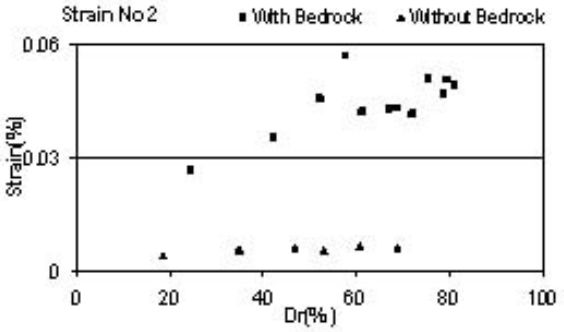

Fig. 35. f=5 Hz, a=0.3 g, buckling mode

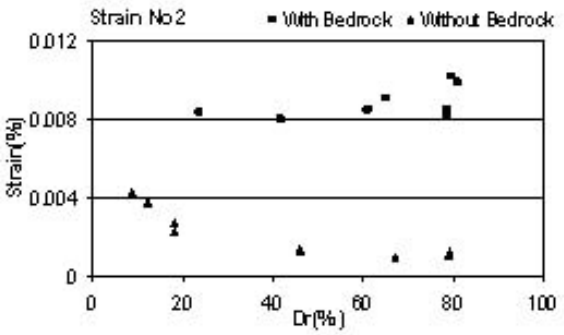

Fig. 36. f =5 Hz, a=0.1g, buckling mode

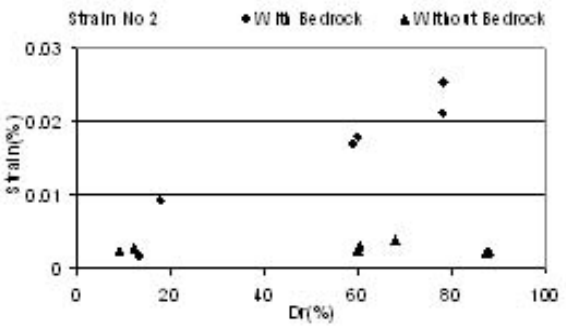

Fig. 37. f =10 Hz, a=0.3 g, buckling mode

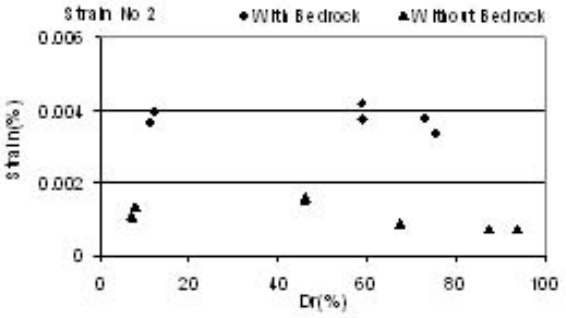

Fig. 38. f =10 Hz, a=0.1g, buckling mode

5. 5. Effect of relative density on pipe strains

In this section the density effect on pipe strains is investigated. The effect is more pronounce if the acceleration possesses higher values. It means that greater values for acceleration will more visibly show the density effect on the pipe deformations. The density effect is more distinctive when it passes through loose region to medium dense one. Conversely, the difference between strains results gets less, when the model density changed from medium to dense condition. Figures 45 to 50 present some

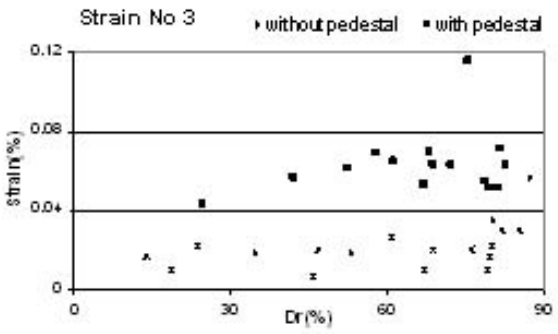

Fig. 39. f=5 Hz-a=0.2-0.5g- Buckling mode

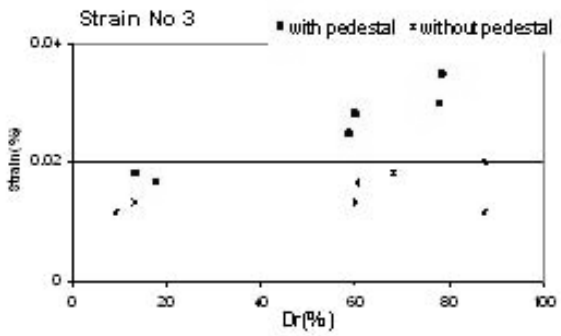

Fig. 40. f=10 Hz-a=0.3g- Buckling mode

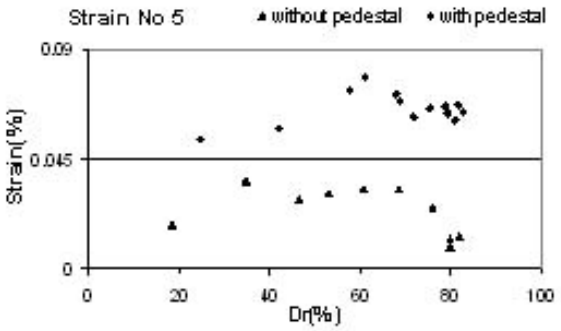

Fig. 41. f=5 Hz-a=0.24g- Buckling mode

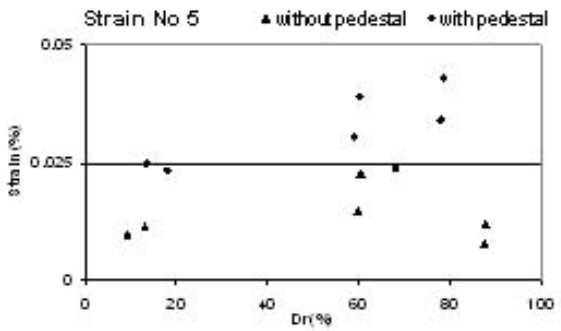

Fig. 42. f=10 Hz, a=0.3g-Buckling mode

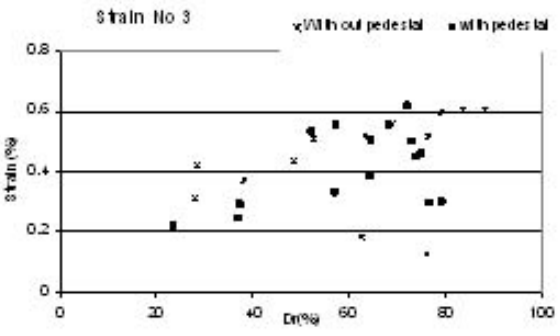

Fig. 43. f=5 Hz-a=0.2-0.4 g – Bending mode

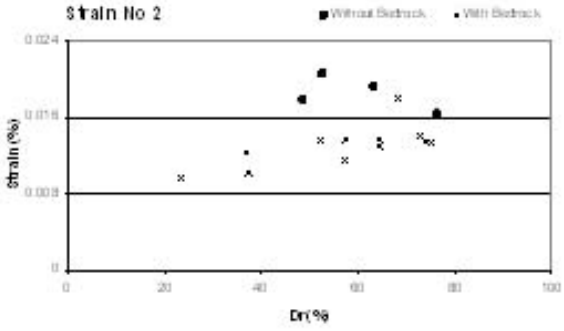

Fig. 44. f=5 Hz-a=0.3 g – Bending mode

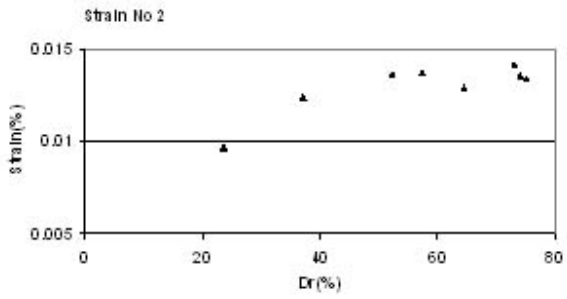

Fig. 45. f=5 Hz-a=0.3 g – bending mode-with pedestal

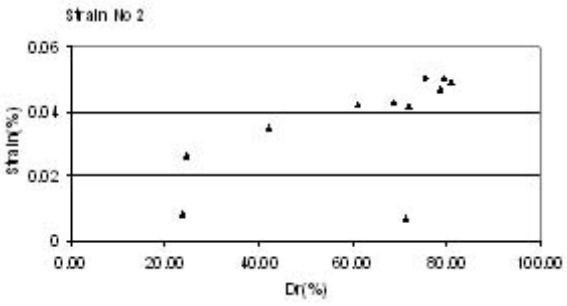

Fig. 46. f=5 Hz-a=0.3 g – buckling mode- with pedestal

examples of measured longitudinal and circumferential strains for the tests. These figures imply that the effect of the relative density on the pipe follow an asymptotic manner after the relative density passes 60%.

5. 6. Effect of Frequency on Pipe Strains

In order to verify the resonance frequency of model including the shear box and its contents, two types of excitation were induced, 5 and 10 Hz. Comparing the results for all strain gauges (longitudinal and circumferential ones) with the same loading characteristics than frequency, it could be concluded that 5 Hz frequency had more destructive effect than the other one. This

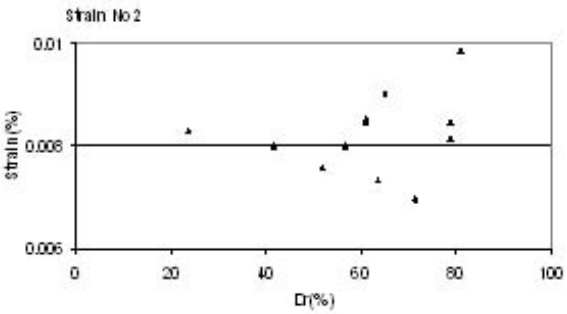

Fig. 47. f=10 Hz-a=0.24 g – bending mode-with pedestal

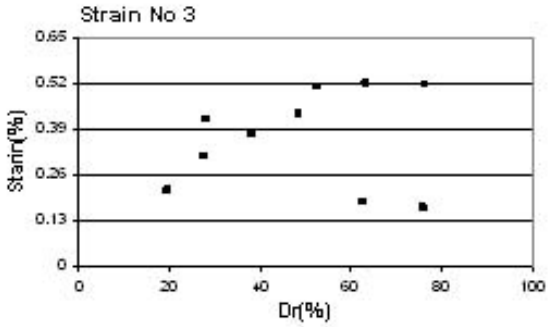

Fig. 48. f= 5 Hz, a=0.2g, bending, without pedestal

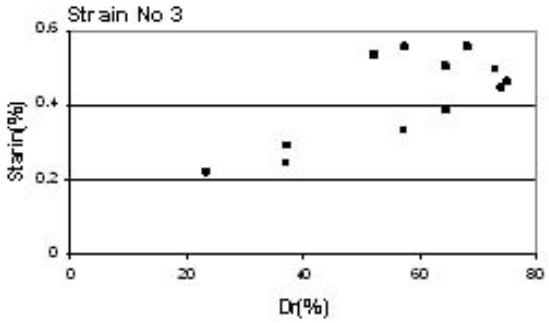

Fig. 49. f= 5 Hz, a=0.3g, bending, with pedestal

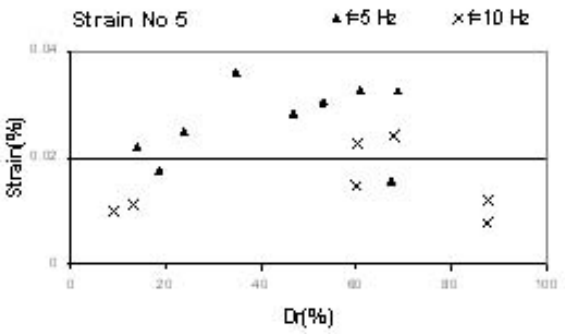

Fig. 50. a=0.3g, buckling, without pedestal

inference is concluded from Figures 51 to 54. These Figures consist of strain records for strain numbers 2, 3 and 5. For each Figure the similar

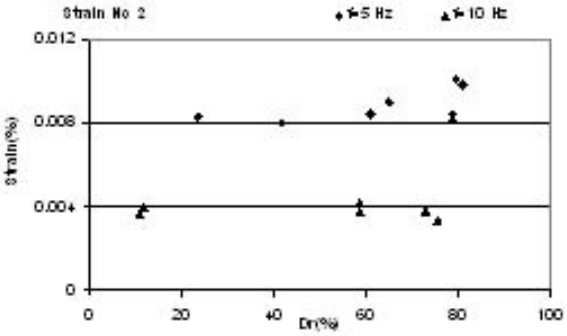

Fig. 51. a=0.1g, Buckling , with pedestal (S2)

loading characteristics such as usage of the pedestal, loading direction and acceleration were chosen. Figures (51) and (52) belong to longitudinal strain; however the others belong to peripheral strains which are strains No. 3 and 5. For all strains shown in these four figures, all strain values related to 5 Hz frequency loading has higher values than the ones with 10 Hz frequency. Although the tests only consisted of two frequencies, it is deduced that 5 Hz frequency is closer to the resonance frequency of whole model.

5. 7. Comparing the peripheral strains along the pipe length

The peripheral strain gauges installed in different lengths of the pipe provided a useful means in investigating the strain distribution on the pipe. Figure 55 compares the two circumferential strains at two different points on the pipe for the model. Since the loading direction was parallel to the pipe axis and the dynamic force did not vary along the pipe, the strains have almost the same values. The same trend is expected in strain points shown in Figure 56. It is noted that each horizontal line depicted parallel to X-direction (in Figures 55 to 58) belongs to an equal loading characteristics. For instance line A (Figure 55) which intersects the two strain points along the pipe length, corresponds to a loading condition with unchanged frequency and acceleration. So, the main objective of this section is to show the independency of peripheral strains to pipe length.

Comparing the recorded strains for the two peripheral strain gauges between the model groups A&B, has led us to relate this difference to

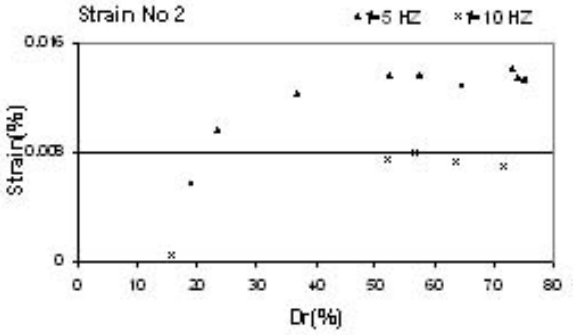

Fig. 52. a=0.3g, Bending, with pedestal(S2)

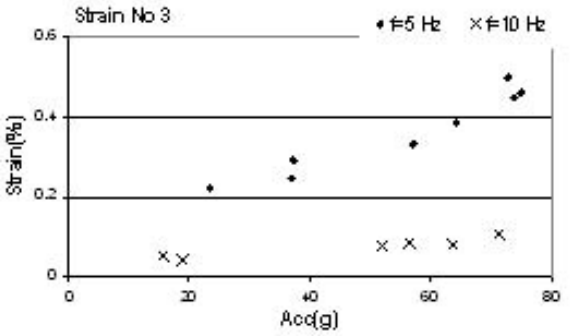

Fig. 53. a=0.3g, Bending, with pedestal (S3)

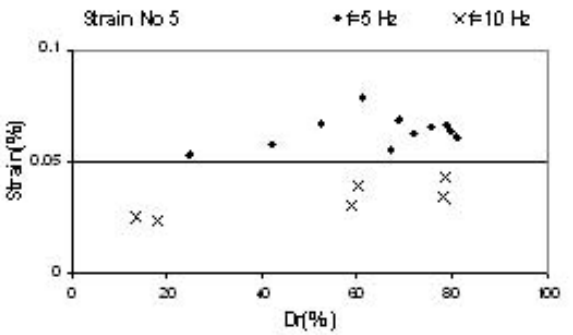

Fig. 54. a=0.3g, Buckling, with pedestal (S5)

loading direction. Yet the strain values at mid-length (strain gauge No. 3) were smaller or at least similar to strains No. 5 in buckling mode, this rule was incorrect in bending one. Because, for loading direction perpendicular to pipe axis, peripheral strains at mid length of the pipe had greater values than ones for strain No. 5. This result which is proved by monitoring the strain points in Figures 57 and 58 for 5 Hz frequency loading and 60 to 500 gal accelerations is due to the fact of strain gauges arrangement on the pipe.

Because the strain gauges No. 3 was installed at the mid length of the pipe, it was induced to more bending force than the strain gauges near the supports. This fact can be probed considering the deformed shape of a beam, induced to forces causing bending moment on it. As discussed in solid mechanics, this situation suggests that a beam with this type of supports must be designed against bending failure for the moment at mid length. This correct issue made us to consider the mid pipe deformations as the critical ones (between two joints) and the mid-length moment as the design moment.

5. 8. Comparison of horizontal strains for soil and pipe

The influence of dynamic loading on the soil and the pipe can be studied by comparing the longitudinal and shear strains on the pipe and the adjacent soil. Figure 59 shows the strain distribution of the pipe and the adjacent soil versus relative density. The ratio of the two strains is illustrated in Figure 60.

The average ratio of strains induced in sand is

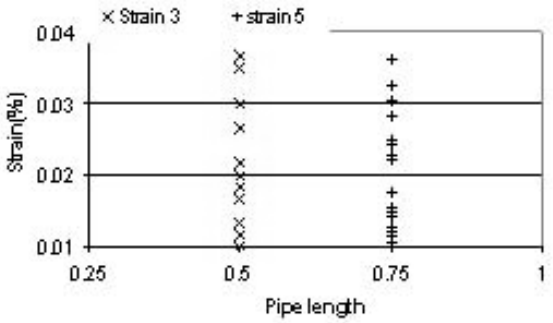

Fig. 55. Peripheral strain distribution along the pipe length f=5-10Hz, a=0.1-0.5g, Buckling, without pedestal

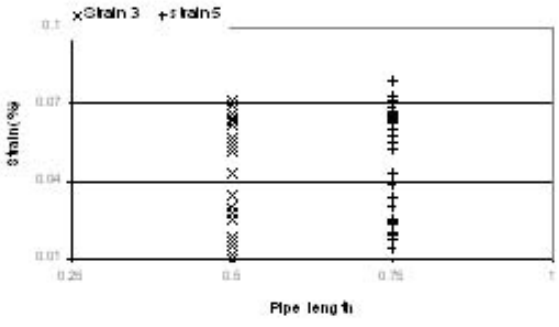

Fig. 56. Peripheral strain distribution along the pipe length f=5-10 Hz, a=0.1-0.4 g, Buckling, with pedestal

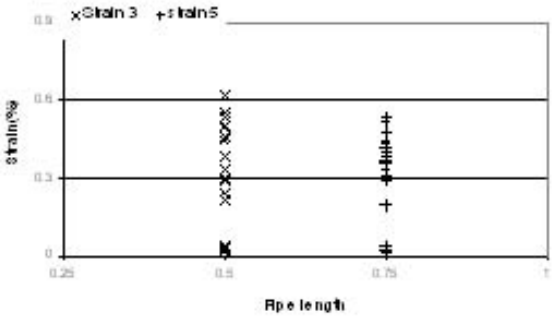

Fig. 57. Peripheral strain distribution along the pipe length-f=5Hz, a=0.1-0.45g, Bending, with pedestal

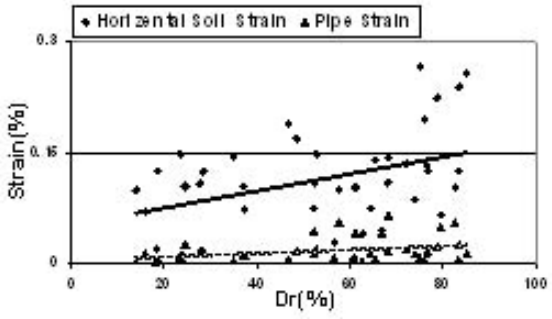

Fig. 59. Comparison of Strains in pipe and soil

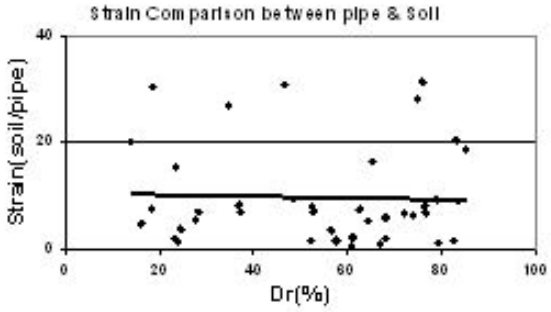

Fig. 60. Ratio of Soil to pipe Strains versus Dr

10 times as much as those on the pipe; however the maximum ratio is 31.2 for Dr=76% and acc=400 gal, while the minimum value is 1 for Dr=60% and acc=100 gal.

The average strains for soil and pipe in loose area are 0.09% and 0.0106%; respectively. These strains increase to 0.1% and 0.0192% for medium dense soil and to 0.15% and 0.025% for dense one.

6. Conclusions

In this paper the dynamic response of a PVC pipe buried in dry sandy soil layer was investigated. The major conclusions are as follows:

1. The Raa (acceleration amplification ratio) values trend to unity as the relative density of the soil approaches 100%. But an evident trend could not be deduced for loose and medium dense soil, since the calculated Raa records consisted of quantities both higher and lower than one.

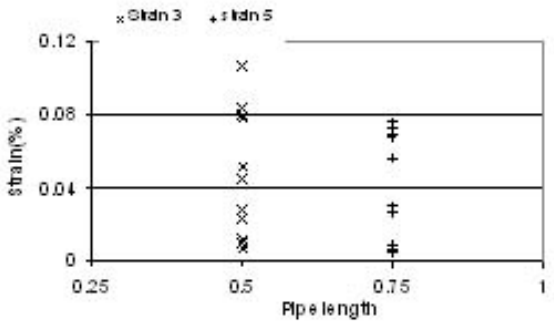

Fig. 58. Peripheral strain distribution along the pipe length f=10Hz, a=0.06-0.25g, Bending, with pedestal

2. Regardless of the frequencies of the experiments, increasing the base acceleration causes more deformations to take place on the pipe.
3. In models containing pedestal, the buckling mode of loading induced higher strains on the pipe than the bending one. On the contrary, if the pedestal was not used, the bending mode is dominant and responsible for causing more deformations than the buckling one.
4. For circumferential strains in all cases including models with and without pedestal, perpendicular loading led to higher strains than the parallel loading. Infer
5. As the density of the soil increases, its effect on the pipe strain diminishes, meaning that the differences between the strains for two similar loading conditions could be more recognized for relative density in loose and medium dense area.; but in dense area, Dr>60%, the density effect on the strains attenuated.
6. Investigating the circumferential strain

distribution on the pipe, it is understood that in bending mode the mid length strains cause the failure to take place, while in buckling mode of loading the longitudinal strains along the pipe are constant.

7. Comparing the strains in soil and pipe, two different materials with different constitutive behavior, shows that the horizontal strains in the soil surrounding the pipe are averagely ten times greater than the ones of the pipe.

References

[1] Ariman T., Lee.: 1991, Tension/Bending Behavior of Buried Pipeline under Large Ground Deformation in Active Faults, NCEER Reports, 91-0001, p489.

[2] Tohada J., Le L., Hamada T., Law H., Ko H.: 1995, Measurement of Strain Distribution Along a Buried Pipeline under Seismic Loading in Centrifuge Models, Proceeding of Earthquake Geotechnical Engineering, Balkema, Rotterdam.

[3] Miyajima M., Yashida M., Kitaura M.:1992, Small Scale Test on Countermeasure against Liquefaction for Pipeline Using Gravel Drain System, NCEER Reports,92-0019, p381.

[4] Towhata I., W.Vargas-Monge, Orense R., Yao M.: 1999, Shaking Table Tests on Subgrade Reaction of Pipe Embedded in Sandy Liquefied Subsoil, Journal of Soil dynamics and Earthquake Engineering 18, pp.347-361.

[5] Kiku , Yasuda S. , Nagase H.:1995, Shaking table tests and several analyses on the behavior of buried pipes during liquefaction , Proceeding of Earthquake Geotechnical Engineering, Balkema, Rotterdam.

[6] Yanagimoto H., Ono T., Yasuda S., Kiko H.: 1992, Several Simulation of Buried Pipeline During Liquefaction, NCEER Reports,92-0019, p453.

[7] Yasuda S., Nagase H., Itafuji S., Sawada H., Mine K.: 1994, Shaking Table Test on Floatation of Buried Pipes Due to Liquefaction of Backfill Sands, NCEER Reports, 94-0026, p665.

[8] J.P. Bardet, C.A. Davis.: 1999, Response of Large Diameter Buried Pipe to Earthquakes, Proceeding of Earthquake Geotechnical Engineering, Balkema, Rotterdam.

[9] O'Rourke T.D., Palmer M.C.: 1994, Earthquake Performance of Gas Transmission Pipelines, NCEER Reports, 94-0026, p679.

[10] Hamada M..: 1991, Estimation of Earthquake Damage to Lifeline Systems in Japan, NCEER Reports, 91-0001, p5.

[11] Y. Mohri,A. Yasuda,T. Kawabata,H.I. Ling.: 1999, Simulation Analyses on Countermeasure Testing for Underground Pipeline" Proceeding of Earthquake Geotechnical Engineering, Balkema, Rotterdam.

[12] Michael J.O'Rourke , Xuejieb Liu.: 1994, Failure Criterion for Buried Pipe Subjected To Longitudinal PGD: Benchmark Case History, NCEER Reports, 94-0026, p639.

[13] Jourabchian, A.: 2002, Designing the laminar shear box for shaking table test, MSc. Thesis, Sharif University of Technology.